D. J. (1990) *Biochemistry 29*, 10855–10864.
Stein, P. E., Leslie, A. G. W., Finch, J. T., Turnell, W. G., McLaughlin, P. J., & Carrell, R. W. (1990) *Nature 347*, 99–102.
Travis, J., & Johnson, D. (1981) *Methods Enzymol. 80*, 745–765.
Wright, H. T., Qian, H. X., & Huber, R. (1990) *J. Mol. Biol. 213*, 513–528.

Thermodynamics of Condensation of Nuclear Chromatin. A Differential Scanning Calorimetry Study of the Salt-Dependent Structural Transitions†

Barbara Cavazza, Gianluigi Brizzolara, Giuseppe Lazzarini, and Eligio Patrone*
Centro di Studi Chimico-Fisici di Macromolecole Sintetiche e Naturali, CNR, 16132 Genova, Italy
Maresa Piccardo, Paola Barboro, Silvio Parodi, Andrea Pasini, and Cecilia Balbi
Istituto Nazionale per la Ricerca sul Cancro, 16132 Genova, Italy
Received May 17, 1991

ABSTRACT: We present a detailed thermodynamic investigation of the conformational transitions of chromatin in calf thymus nuclei. Differential scanning calorimetry was used as the leading method, in combination with infrared spectroscopy, electron microscopy, and techniques for the molecular characterization of chromatin components. The conformational transitions were induced by changes in the counterion concentration. In this way, it was possible to discriminate between the interactions responsible for the folding of the higher order structure and for the coiling of nucleosomal DNA. Our experiments confirm that the denaturation of nuclear chromatin at physiological ionic strength occurs at the level of discrete structural domains, the linker and the core particle, and we were able to rule out that the actual denaturation pattern might be determined by dissociation of the nucleohistone complex and successive migration of free histones toward native regions, as recently suggested. The sequence of the denaturation events is (1) the conformational change of the histone complement at 66 °C, (2) the unstacking of the linker DNA at 74 °C, and (3) the unstacking of the core particle DNA, that can be observed either at 90 or at 107 °C, depending on the degree of condensation of chromatin. Nuclear chromatin unfolds in low-salt buffers, and can be refolded by increasing the ionic strength, in accordance with the well-known behavior of short fragments. The process is athermal, therefore showing that the stability of the higher order structure depends on electrostatic interactions. The transition between the folded conformation and the unfolded one proceeds through an intermediate condensation state, revealed by an endotherm at 101 °C. The analysis of the thermodynamic parameters of denaturation of the polynucleosomal chain demonstrates that the wrapping of the DNA around the histone octamer involves a large energy change. The most striking observation concerns the linker segment, which melts a few degrees below the peak temperature of naked DNA. This finding is in line with previous thermal denaturation investigations on isolated chromatin at low ionic strength, and suggests that a progressive destabilization of the linker occurs in the course of the salt-induced coiling of DNA in the nucleosome.

In a recent paper (Balbi et al., 1989), we reported on a differential scanning calorimetry (DSC)[1] study of chromatin within rat liver nuclei. Between 70 and 110 °C, the thermal profile of this material showed three main, well-separated endotherms (Nicolini et al., 1983; Balbi et al., 1989), and we sought their relationship to the melting of the structural domains of the polynucleosomal chain. The thermal peaks observed at 68 and 85 °C for micrococcal nuclease digested nuclei were attributed to the linker and core particle DNA; more importantly, for native material, the major heat investments occurred at 107 and 90 °C. Since the equilibrium unfolding of the higher order structure resulted in the transfer of denaturation heat from the former endotherm to the latter (Balbi et al., 1988, 1989), we concluded that DSC can be regarded as a leading method for investigating the conformational changes underlying transcription and replication. Besides this perspective, the calorimetric approach can be extended in order to assess the role of condensation phenomena in gene regulation. Indeed, a DSC characterization of the organization of chromatin in transformed rat hepatocytes (Balbi et al., 1990) revealed the occurrence of an extensive decondensation process, and we were in consequence struck by the identification of a protein responsible for the packaging of the chromatin fiber into heterochromatin in position-effect variegation (Reuter et al., 1990).

† This work was supported by the Italian National Research Council, Special Project "Oncology" (Grant 104348.44.8808213), and the EEC [Grant EV4V-0036-I(A)]. M.P. thanks the Italian Association for Cancer Research for a fellowship.
* Correspondence should be addressed to this author at the Centro di Studi Chimico-Fisici di Macromolecole Sintetiche e Naturali, Corso Europa 30, 16132 Genova, Italy.

[1] Abbreviations: DSC, differential scanning calorimetry; IR, infrared; mol bp, moles of base pairs; DM, dissociation medium; EDTA, ethylenediaminetetraacetic acid; PMSF, phenylmethanesulfonyl fluoride; Tris, tris(hydroxymethyl)aminomethane; SDS, sodium dodecyl sulfate; kDa, kilodalton(s); kb, kilobase(s); DNase, deoxyribonuclease.

0006-2960/91/0430-9060$02.50/0

The quantitative treatment of the results is, however, the necessary counterpart of the calorimetric approach to the conformational changes in nuclei, and several questions still remain unanswered concerning (1) the thermodynamics of the decondensation process as well as (2) the contributions of the chromatin components to the denaturation of the structural domains. There are very few, conflicting reports in the literature (Weischet et al., 1978; Bina et al., 1980) on the nature of the forces responsible for the stability of the nucleosome. Early experiments on the unfolding of the core particle (Weischet et al., 1978) showed that ~100 base pairs of DNA, which are stabilized by the interaction with the histone octamer, have a denaturation enthalpy of 12.2 kcal·(mol bp)$^{-1}$, which is well above the value of unprotected DNA. Therefore, it could be deduced that hydrogen bonds contribute to the stability of the domain. In contrast, Bina et al. (1980) compared the denaturation enthalpy of the core particle with those of the histone octamer and of the core particle DNA and concluded that the formation of the complex is entirely entropy-driven, in accordance with the predictions of the polyelectrolyte theory (Record et al., 1976). The same uncertainty exists with regard to the folding of the polynucleosomal chain into the higher order structure. Morphological evidence has been presented in favor of a purely electrostatic mechanism (Widom, 1986). When nuclear chromatin is extensively digested with micrococcal nuclease, the total transition enthalpy decreases (Balbi et al., 1989), suggesting the existence of an enthalpic contribution to the stability of the ordered state. The decondensation induced by ethidium intercalation is, however, athermal (Balbi et al., 1988, 1989). In this paper, we present a calorimetric study of the cyclic decondensation–condensation process induced by changing the ionic strength of the solvent medium, which allows us in a straightforward manner to measure the energetics of folding. These experiments demonstrate a major involvment of salt linkages with respect to other sources of stabilization.

The second important question concerns the actual relationship between the unfolding of histones and the unstacking of DNA. The answer can be obtained by developing spectroscopic methods suitable for monitoring the conformational changes of these components. In a classical paper, Weischet et al. (1978), by relating the temperature dependence of the ellipticities at 223 and 273 nm with the excess heat capacity curve, were able to demonstrate that in low-salt buffer, the core particle denatures almost cooperatively. Such an exhaustive analysis could not be further pursued since, at physiological ionic strength, the high turbidity of the chromatin suspensions prevents the use of both circular dichroism and hyperchromicity at 260 nm. As will be shown in the following, infrared (IR) spectroscopy in the 1400–1700 cm^{-1} region yields an accurate representation of the melting of histones and of DNA. In partially digested nuclei, the histone complement unfolds in a broad transition centered around 68 °C, while the DNA unstacks at 73 and 87 °C, in accordance with our previous assignments (Balbi et al., 1989). The comparison with the calorimetric data revealed important features of the polynucleosomal chain assembly. The linker domain, indeed, appears to be less stable than "free" DNA for counterion concentrations higher than 30 mM. This behavior reflects subtle conformational aspects of nucleosome positioning, which escaped current observation methods.

In our previous investigations, the DSC experiments were carried out on rat liver nuclei. As already noted, activation of endogenous nuclease occurs in this material at low ionic strength, and can result in the extensive digestion of chromatin. Furthermore, an appreciable amount of intermediate filaments remains firmly bound to the nuclear lamina even if careful purification protocols are used. These contaminants melt together with the components of the nuclear matrix between 40 and 70 °C, and make the unambiguous determination of the denaturation curve of histones difficult. Owing to a higher stability, and to the low content of non-histone proteins, calf thymus nuclei were used in the present work with a view of developing a comprehensive thermodynamic analysis.

Experimental Procedures

Preparation and Characterization of Nuclei from Calf Thymus. Nuclei were isolated from calf thymus by a modification of the method described previously (Cavazza et al., 1983). During preliminary experiments, we noticed that the activity of endogenous proteases and nucleases could be suppressed almost completely by performing both the grinding and the washing steps in dissociation medium (DM) (75 mM NaCl, 24 mM Na_2EDTA, 5 mM $NaHSO_3$, and 1 mM PMSF, pH 7.8) which was therefore used instead of the low-salt buffer (0.25 M sucrose, 10 mM Tris, and 5 mM $MgCl_2$, pH 8). All the preparative steps were carried out at 4 °C. Twenty grams of frozen tissue was cut into small pieces and homogenized in a Waring blender with 300 mL of DM. The crude suspension was filtered through six layers of sterile gauze, and an equal volume of DM containing 0.6% (v/v) Triton X-100 was added under gentle shaking. After a 5-min incubation, nuclei were harvested by centrifuging at 500*g* for 10 min and resuspended in DM; this washing step was repeated 3 more times. Purified nuclei were recovered by centrifugation at 10000*g* for 15 min. The material prepared according to this improved protocol was stable for several days when stored at 4 °C, as judged from both the DSC profile and the electrophoretic pattern of histones and DNA on SDS–polyacrylamide and agarose gels, respectively. Rat liver nuclei were isolated in flow according to the method by Balbi et al. (1989). The chemical assay of DNA, RNA, and proteins was performed as already reported (Balbi et al., 1989).

Preparation of Unfolded and Refolded Nuclear Chromatin. The unfolding of the higher order structure was induced by dispersing the nuclear pellet in a large excess of dilute DM (Na^+ concentration from 20 to 1 mM) at 4 °C. After a 10-min incubation, nuclei were recovered by centrifugation at 500*g* for 3 min. This washing step was repeated twice more, and the pellet was incubated at 25 °C for different lengths of time (15 and 30 min). Nuclei exposed to 10 mM Na^+ for 30 min were renatured by exhaustive dialysis against DM at 25 °C. Samples for DSC experiments were obtained by centrifugation at 10000*g* for 10 min. Chromatin fragments were isolated by disrupting the nuclear pellet with three strokes in a tight-fitting Dounce homogenizer. The suspensions were centrifuged at 10000*g* for 20 min, and the supernatants, containing 10 μg/mL DNA, were used for observations in the electron microscope by a standard procedure as described below.

Chromatin was irreversibly decondensed by extensive digestion of nuclei with trypsin according to Allan et al. (1982). Nuclei were resuspended in DM at a concentration of ~0.2 mg/mL and digested with 20 μg/mL trypsin (type 8642, Sigma) for 1 h at 4 °C. The reaction was stopped by adding a 4-fold excess of soybean trypsin inhibitor (type 9003, Sigma). The pellet was washed twice with an excess of DM in order to remove the enzyme and the inhibitor.

Dissociation of Nuclear Chromatin at High Ionic Strength. Chromatin was dissociated by adding to a known amount of nuclear pellet in DM an equal volume of the same buffer

containing 4 M NaCl. After overnight dialysis against a large excess of 2 M NaCl in DM, aliquots of the resulting homogeneous gel were directly transferred to the calorimetric capsules.

Preparation of Thermally Denatured Chromatin for Electron Microscopy. Calf thymus nuclei were resuspended in 75 mM NaCl, 1 mM $CaCl_2$, and 2.5 mM Tris (pH 8) at a DNA concentration of 2–3 mg/mL and digested with 50 units/mL micrococcal nuclease (Sigma) for 60 min at 37 °C. The reaction was stopped by adding 4 volumes of DM. Nuclei were recovered by centrifugation at 10000*g* for 10 min, and after another washing step in the same buffer, they were thermally denatured at a scan rate of 10 °C/min. The calorimetric capsules were cooled in the calorimeter at rate of 100 °C/min and opened, and the denatured nuclear pellet (50 mg) was extracted overnight at 4 °C with 0.50 mL of DM. Prior to the mounting for electron microscopy, gross nuclear debris were removed by brief centrifugation at 5000*g*.

Electron Microscopy. A droplet of chromatin suspension was applied to a carbon-coated grid for 15 min, the excess removed by filter paper, and the adsorbed material negatively stained with 1% uranyl acetate. Thermally denatured chromatin was also visualized by the phospholipid monolayer technique, as already described (Cavazza et al., 1983; Balbi et al., 1989). A Siemens 102 electron microscope operating at 80 kV was used.

Isolation and Gel Electrophoresis of DNA, Nuclear Proteins, and Whole Histones. DNA was isolated by digestion of calf thymus nuclei with proteinase K (Serva) followed by extraction with phenol and chloroform (Maniatis et al., 1982) and electrophoresed on agarose gels as already reported (Balbi et al., 1989). Electrophoresis on alkaline 1.5% agarose gels was carried out according to Maniatis et al. (1982). The gels were stained with 1 μg/mL ethidium bromide. Alkaline gels were soaked for 1 h in neutralizing solution (1.5 M NaCl, 1 M Tris, pH 7.6) prior to being stained.

Total nuclear proteins were solubilized by overnight extraction of 100 mg of pelleted calf thymus or rat liver nuclei with 1 mL of 0.125 M Tris (pH 6.8) containing 5% SDS. After centrifugation at 10000*g* for 15 min, the supernatant was analyzed by SDS–polyacrylamide electrophoresis. Histones were obtained by acid extraction of nuclei followed by ethanol precipitation (Panyim et al., 1971). Total nuclear proteins and histones were run on 8–15% gradient and on 15% SDS–polyacrylamide gels, respectively, according to Laemmli (1979).

IR Spectroscopy. D_2O buffer (0.122 M NaCl, 0.5 mM Na_2EDTA, and 10 mM Tris, pH meter reading 7) was prepared by adding under vacuum, to weighed amounts of the salts (total weight 0.09 g), a 0.5-mL aliquot of D_2O (Fluka, purity better than 99.8%). The mixture was dissolved by heating at 45 °C, and D_2O was removed at the vacuum pump. This operation was repeated several times, in order to achieve the complete exchange of protons; the progress of the exchange was checked by measuring the absorption of HOD at 1455 cm^{-1}. D_2O was then added up to the required volume, and nuclei were deuterated in a drybox fluxed with nitrogen by resuspending the pellet in a large volume of D_2O buffer for 1 h. The sedimented nuclei were recovered by decantation. After six changes of the buffer, the pellet was transferred to a variable-temperature cell (Specac Model 20500) with CaF_2 windows (optical path length 25 μm), and the spectra were run over the frequency range 1400–1700 cm^{-1} in a Perkin-Elmer Model 983 grating spectrophotometer equipped with a Specac automatic temperature controller P/N 20120.

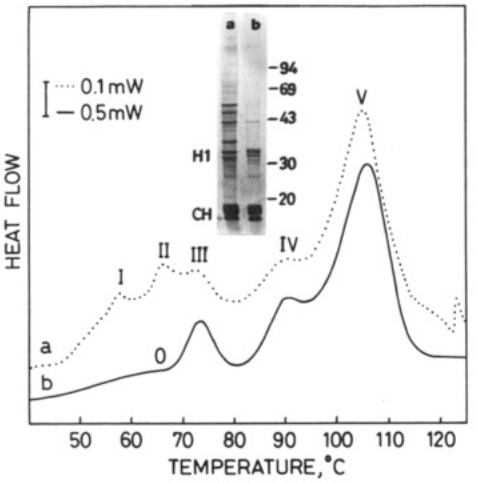

FIGURE 1: Comparison between the thermal profile of rat liver (scan a) and calf thymus nuclei (scan b) in DM. The electrophoretic characterization of total nuclear proteins on 8–15% gradient SDS–polyacrylamide gels is shown (lanes a and b). Histones are designated by H1 and CH (core histones). The molecular weight of standard proteins ($\times 10^{-3}$) is reported on the right.

Thermal denaturation was carried out at the same heating rate used in the DSC experiments (10 °C/min). The absorption of the solvent was recorded at each temperature and subtracted to the spectrum of nuclei on a Perkin-Elmer 7500 computer. The data from five experiments, in the form of percent hyperchromicity at 1439 or 1625 cm^{-1}, were fit by the Enzfitter program on a IBM PC using a single or two hyperbolic tangent functions. The derivative was deconvolved into Gaussian component transitions as described below.

Calorimetry. DSC experiments were carried out as already described (Balbi et al., 1989). However, in order to minimize the interference of thermal degradation of DNA, the experiments were carried out at a higher scan rate (10 °C/min). This change neither affected the reliability of the measurement nor worsened the resolution of fine thermal effects, as judged by both the values of the thermodynamic parameters of denaturation of standard proteins (ribonuclease and lysozyme) and the melting profile of DNA from calf thymus. Deconvolution of the excess heat capacity curves and of the derivative melting profiles was performed by an optimized computer program written by Dr. E. Freire.

Results and Discussion

Domain Model of Thermal Denaturation of Chromatin. Short Reexamination of the Problem by a Calorimetric Criterion. In order to link up our previous observations (Balbi et al., 1989) and the present analysis of the melting of chromatin, in Figure 1 we compare the thermograms of purified nuclei from rat liver and calf thymus (scans a and b, respectively). The major endotherms are marked by Roman numerals. Transitions III, IV, and V are due to the unstacking of the nucleosomal DNA belonging to different structural domains. The assignments to the linker DNA (III), to core particle DNA when the core particles do not substantially interact (IV), and to core particle DNA belonging to clustered, interacting core particles (V) have already been discussed. Above 70 °C, the thermal profiles are superimposable. The dominance of transition V is related to the functional state of the nucleus, namely, the large value of ΔH_m^V indicates that most of the chromatin is in the condensed state, as expected for cells from mature tissues (Balbi et al., 1989).

Major differences are observed in the low-temperature region. Transitions I and II, which are prominent in the ther-

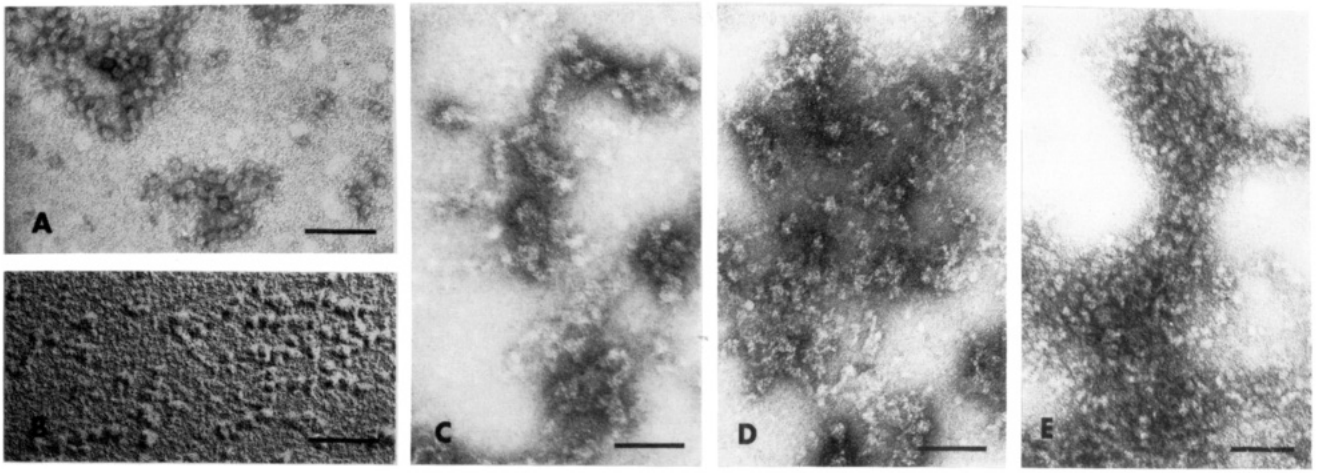

FIGURE 2: Effect of thermal denaturation and of changes in the counterion concentration on the morphology of chromatin isolated from calf thymus nuclei. (A, B) Chromatin from nuclei digested with 50 units/mL micrococcal nuclease for 15 min, and thermally denatured up to 125 °C at a scan rate of 10 °C/min. (C) Native chromatin from nuclei in DM. (D) Unfolded chromatin from nuclei exposed to dilute DM (10 mM Na^+) for 30 min at 25 °C. (E) Refolded chromatin from nuclei treated as in (D) and dialyzed against DM. All the specimens were negatively stained with uranyl acetate except (B), which was adsorbed onto a phospholipid monolayer and shadowed with platinum. The bar is 0.1 μm.

mogram of rat liver nuclei (scan a), are no longer observed in the case of calf thymus (scan b). This discrepancy is by no means surprising, since these endotherms arise from the denaturation of scaffolding structures, which, in rat liver nuclei, appear to be associated with an appreciable amount of intermediate filaments. Even the improved isolation procedure used in this work yields a material having a DNA:non-histone proteins ratio of the order of 1.3. This value raises to 25 for calf thymus nuclei, which is in line with a previous estimate (Mirsky, 1971). The electrophoretic patterns of the total nuclear proteins (see Experimental Procedures) on SDS–polyacrylamide gels are shown in the inset; the amounts loaded onto the gels correspond to 1 mg of DNA. In the case of rat liver (lane a), at variance with calf thymus nuclei (lane b), we observe three heavily stained bands at 54, 47, and 43 kDa, corresponding to components of the intermediate filaments. The densitometry of the gels shows that the amount of non-histone proteins is 20 times larger for the former material, in agreement with the chemical assay. The absence of a significant interference of the melting of scaffolding structures allows us to search for eventual transitions of chromatin occurring below 70 °C. Interestingly, a broad endotherm centered around 66 °C is apparent in scan b. In order to maintain our previous notation, it is referred to here as 0.

Before we proceed to a comprehensive treatment of the results, a few comments with regard to the mechanism of denaturation of chromatin are necessary. The DSC approach builds on the same assumption underlying previous thermal denaturation studies, namely, that no appreciable dissociation of histones from DNA occurs during the experiment (Li, 1977), so that the denaturation of energetically distinguishable domains is directly reflected in the thermal profile. Other workers (Almagore & Cole, 1987, 1989a) have interpreted endotherms IV and V as being actually related to the unstacking of supercoiled and relaxed DNA, rather than to its denaturation within the core particle. For supercoiling to be detectable, however, the nucleohistone complex must undergo dissociation upon heating. Such a circumstance should have seriously challenged the reliability of thermal denaturation studies and, of course, has never been registered. It has been noted earlier that the core particle undergoes a morphological rearrangement when heated up to the temperature of the main transition of the DNA (Seligy & Poon, 1978). Sliding of the histone octamer possibly occurs during the thermal denaturation of H1-depleted chromatin at low ionic strength (Tsaneva et al., 1980; Dimitrov et al., 1980). These reports, however, do confirm that not even under the conditions of extreme destabilization of the complex (which resulted from the removal of H1) are core histones released from chromatin. The micrograph in Figure 2A shows the morphology of chromatin fragments extracted from calf thymus nuclei digested with micrococcal nuclease and submitted to thermal denaturation up to 125 °C at a scan rate of 10 °C/min. After complete unstacking of the DNA, the core particles are still visible as negatively stained particles 11.3 ± 0.22 nm (mean ± standard deviation) in diameter. The occurrence of some limited molecular rearrangement is suggested by the absence of penetration of the stain into the core protein, which gives the native fiber an irregular, knobby appearance. A similar beaded morphology can be seen when the specimen is adsorbed onto a phospholipid monolayer and shadowed with platinum (Figure 2B). The experiments described below provide additional information on the denaturation mode of native chromatin at physiological ionic strength.

Calf thymus nuclei were scanned up to 125 °C at a rate of 10 °C/min (solid line in Figure 3). Another aliquot of the pellet was scanned up to the temperature indicated by an arrow (dashed line), cooled in the calorimeter at a high cooling rate (100 °C/min) down to 25 °C, and rescanned as the reference sample (dotted line). It can be seen that all the transitions are irreversible, except for IV that exhibits a partial reversibility. It is apparent, however, that the denaturation of a given domain neither affects its temperature and enthalpy of melting nor appreciably perturbs the melting of native regions. For example, in experiment a, the sample was heated up to T_m^{III} (74 °C). In the successive scan, the transition is still observed at this temperature, while ΔH_m^{III} halves. All the other endotherms do not undergo significant alterations. In this experiment, due to the fact that the amounts of chromatin used in the reference and in the successive scans were slightly different, the trend of the transition enthalpies cannot be fully appreciated on visual inspection of the thermograms. The steadiness of ΔH_m^{IV} and ΔH_m^{V}, however, has been verified by deconvolution of the excess heat capacity curves, as described below. The same behavior can be observed when the first scan is stopped at 100 (b) and 107 °C (c). In every case, we observe a loss of transition enthalpy only which corresponds to the amount of irreversibly denatured material. It is clear that

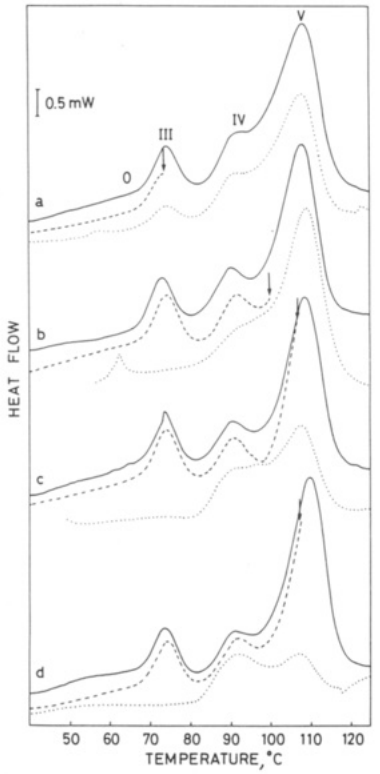

FIGURE 3: Partial thermal denaturation of chromatin does not affect the stability of the domains which are still in the native state. Calf thymus nuclei in DM were heated up to the temperature marked by an arrow at a scan rate of 10 °C/min (dashed line), cooled in the calorimeter down to 15 °C, and rescanned up to 125 °C (dotted line). The reference scan is shown (solid line). The cooling rate is 100 °C/min in (a), (b), and (c), and 10 °C/min in (d).

chromatin melts in independent transitions. The adjective "independent" is used here in an empirical meaning, to denote the absence of secondary effects during the denaturation process.

Apparently this conclusion does not hold when the sample remains for a sufficiently long time at high temperature. In (d), the scan was stopped at 107 °C as in (c), but cooling was performed at a low rate (10 °C/min). In this case, the residual enthalpy of transition V is only 25% of the initial value. This result has two possible explanations. (1) The denaturation of the domain is followed by a slower rearrangement of denatured histones, which can therefore migrate toward and bind to native regions causing them to unfold. (2) At high temperature, an appreciable amount of structural defects is introduced into the DNA molecule, leading to the collapse of the higher order structure. Indeed, the destabilizing effect of a limited number of single- or double-strand cuts as well as of methylation has already been documented (Trefiletti et al., 1984; Touchette & Cole, 1985). In order to establish whether a link exists between the enthalpy loss of transition V and DNA damage, nuclei were scanned up to 125 °C at 10 or 1 °C/min and rapidly cooled down to 25 °C, and the extracted DNA was run on alkaline 1.5% agarose gels. The result is shown in Figure 4. The former experiment involves only limited chain scission, since the most probable chain length of the fragments is 6.7 kb (lane a). At the lower scan rate (lane b), however, the frequency of single-strand breaks is as high as 1 per 2 kb, a figure which is compatible with an earlier estimate of the kinetics of cleavage of the phosphodiester bond at 100 °C (Rice & Doty, 1957). The corresponding thermal profile (scan b) shows dramatic alterations. T_m^{III} decreases from 74 to 71 °C, while transition IV is at 88 °C, and merges with a long tail due to degraded material. The experiment

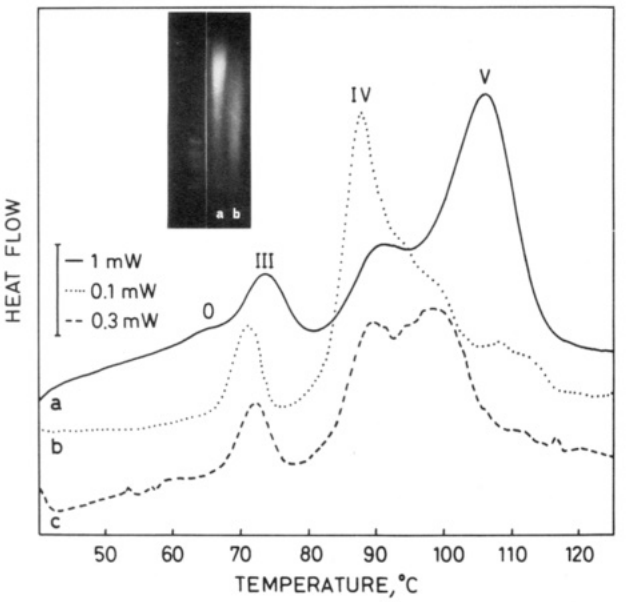

FIGURE 4: Effect of the scan rate on the thermal profile of calf thymus nuclei in relation to DNA chain scission. The electrophoretic patterns of DNA on alkaline agarose gels are shown in the inset. Scan a and lane a, 10 °C/min. Scan b and lane b, 1 °C/min. Scan c, 3 °C/min. Size markers are λ/*Hin*dIII and φX174/*Hae*III fragments.

carried out at 3 °C/min (scan c) indicates that this scan rate is still too low for a reliable determination of the thermal effects occurring in the high-temperature region. It could be objected that this result lends itself to a different interpretation, since DNA undergoes depurination upon heating, and at the apurinic sites the phosphodiester bond is readily hydrolyzed by exposure to alkali. However, using the DNA from φX174, it has been shown that, even under neutral conditions, above 70 °C depurination is followed by chain scission (Fiers & Sinsheimer, 1962).

We conclude that when chromatin is kept at elevated temperatures for extended periods the higher order structure can be lost as a consequence of DNA degradation (it is likely that the histone molecules are extensively damaged as well), so that the DSC experiment can fail to detect major structural aspects. In the absence of an estimate of the frequency of DNA breaks, the incidence of thermal degradation can be ascertained by carrying out determinations at different scan rates.

Experimental Behavior of Nuclear Chromatin in Response to Changes in Counterion Concentration. Phenomenology of the Conformational Transition. As already pointed out, the isolation of nuclei in DM yields a stable material which is suitable for quantitative work, and in Figure 5A we compare three representative scans relative to different preparations. As a rule, the thermal profiles are well consistent (scans b and c), but in a few cases, exemplified by scan a, the ratio of the enthalpies of endotherms IV and V is somewhat lower, as apparent after deconvolution into component transitions. Since the occurrence of degradation processes was systematically ruled out, this minor variability probably reflects fluctuations in the functional state of the tissue. Indeed, it is well-known that calf thymus is derived from stressed animals, a circumstance which can induce degeneration of the gland and cellular changes (Johns et al., 1977).

An example of deconvolution of the excess heat capacity curve, expressed in kilocalories per degrees kelvin per moles of base pairs, relative to scan b, is given in Figure 5B. Except for the low-temperature region, in which transition 0 is clearly resolved, with regard to the melting of DNA we obtain the same representation derived from previous experiments on rat

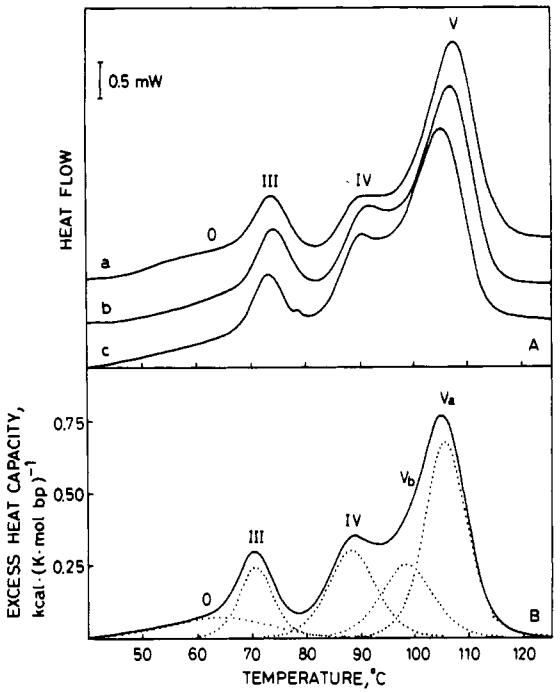

FIGURE 5: (A) Comparison among the thermal profiles of calf thymus nuclei in DM from different preparations. (B) Example of deconvolved excess heat capacity curve. Note that endotherm V is resolved into two components at 101 and 107 °C, respectively.

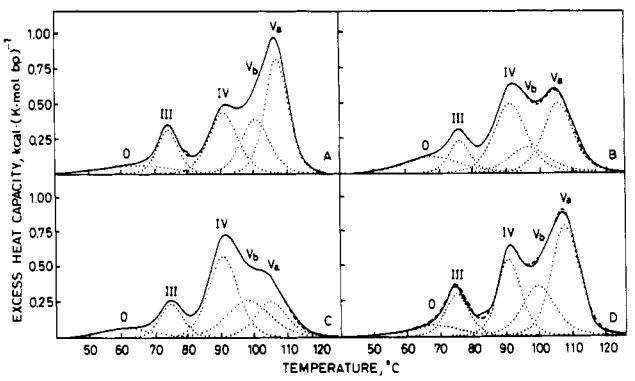

FIGURE 6: Conformational transition of nuclear calf thymus chromatin induced by changes in the counterion concentration. Nuclei in DM (A) were resuspended in dilute DM (10 mM Na^+) at 25 °C for 15 or 30 min and the calorimetric scans performed immediately after (B and C). Refolding of chromatin was achieved by dialysis of the unfolded material (C) against DM; the thermal profile is reported in (D). The corresponding morphologies of the chromatin fibers are shown in Figure 2. Scan rate, 10 °C/min.

liver nuclei. The higher accuracy of the present determinations, however, allows us to further decompose transition V in to two subcomponents at 107 and 101 °C. They will be referred to here as V_a and V_b.

Chromatin can be unfolded and refolded by varying the concentration of Na^+, the onset of condensation being, in the absence of divalent cations, close to 50 mM (Widom, 1986). In the experiments described here, nuclei were submitted to a cyclic change of the ionic strength, and the melting behavior related with the morphology of the chromatin fiber, as visualized in the electron microscope by the negative staining technique. We start with native nuclei in DM (Figure 6A). When the Na^+ concentration is lowered to 10 mM at 25 °C (see Experimental Procedures), we observe a time-dependent decrease in $\Delta H_m^{V_a}$ and $\Delta H_m^{V_b}$, together with a compensating increase in ΔH_m^{IV}; the thermogram in Figure 6B was obtained 15 min after resuspension in the low ionic strength buffer. The drift in the thermal profile is close to completion after 30 min. At that time, much of the heat invested in transition V_a is quantitatively "pumped" in transitions V_b and IV, which now dominate the thermogram (C). Finally, unfolded chromatin was exhaustively dialyzed against DM; the profile of native nuclei is regained (D). Thus, in these experiments, nuclear chromatin undergoes a reversible conformational change, which is expected to be related to the decondensation of tightly packed 30-nm fibers (Widom, 1986). This correspondence has been verified by inspection in the electron microscope of large chromatin fragments released from disrupted nuclei. In the case of native material (Figure 2C), we observe thick fibers, which show local uncoiling, conforming to the coiled-coil or ropelike model for the higher order structure (Cavazza et al., 1983). Thirty minutes after equilibration in 10 mM Na^+, chromatin is found in the extended form (D), which after dialysis takes on the morphology characteristic of the native state (E).

These experiments, which are in remarkable agreement with previous results on the decondensation of chromatin in rat liver nuclei induced by ethidium bromide intercalation (Balbi et al., 1988), will be reconsidered in the next section, with the purpose of attaining a quantitative picture of the energetics of the conformational change. However, a few qualitative features, with direct bearing on the mechanistic interpretation, deserve concise comment. In the present experimental conditions, the decay of the condensed state is characterized by a relaxation time on the order of several minutes. Such a high value is obviously related to the enormous number of linked particles (the nucleosomes) which must undergo a coordinate motion during the decondensation of the bulk of nuclear chromatin. Therefore, by use of straightforward methods of molecular dynamics, the measurement of the relaxation time can give the actual size of the structural unit of the interphase genome, the chromatin loop, for which only indirect estimates are available. Subtransitions V_a and V_b are due to the melting of two different populations of core particles buried within heterochromatin domains differing in the average density, and their decay further characterizes the dynamics of decondensation. For example, the data shown in Figure 6 suggest that the passage of transition enthalpy into transition IV is roughly described by two consecutive reactions; the looser domains melting in V_b undergo a fast decondensation [compare (B) with (A)], while the unfolding of denser chromatin proceeds more slowly from V_a to V_b. Although crude, this picture of the organization of nuclear chromatin can be considered to closely approach any real situation. The structural changes registered during the aging of cell cultures obey the kinetics of consecutive reactions, an intermediate state occurring, as in the present experiments, between 95 and 102 °C (Almagore & Cole, 1989a), and it is worth noting that isolated fragments can be observed, after refolding, in two fairly well-separated levels of compaction (Widom, 1986).

Other workers have recently presented, in a series of related papers, the results of a DSC investigation on nuclei isolated from different cell lines submitted to a variety of physical or biochemical treatments in vitro. The loss of the capacity to divide in nutrient-deprived cells (Almagor & Cole, 1987), the aging and UV irradiation of cell cultures (Almagor & Cole, 1989a), and the effect of anticancer drugs on human epithelial cells (Almagor & Cole, 1989b) were characterized in terms of changes in the structure of chromatin. In all these experiments, a decrease in the enthalpy at 105 °C with respect to the controls was observed. The interpretation of this recurring phenomenon was, however, at variance with the present one. Recalling that the thermal denaturation of supercoiled

Table I: Thermodynamic Parameters for the Melting of Native, Unfolded, and Refolded Nuclear Chromatin from Calf Thymus

	ΔH^0_m [kcal·(mol bp)$^{-1}$]	T^0_m (°C)	ΔH^{III}_m [kcal·(mol bp)$^{-1}$]	T^{III}_m (°C)	ΔH^{IV}_m [kcal·(mol bp)$^{-1}$]	T^{IV}_m (°C)	$\Delta H^{V_b}_m$ [kcal·(mol bp)$^{-1}$]	$T^{V_b}_m$ (°C)	$\Delta H^{V_a}_m$ [kcal·(mol bp)$^{-1}$]	$T^{V_a}_m$ (°C)
native chromatin in DM[a]	2.0 ± 0.5	66.2 ± 1.6	1.9 ± 0.3	73.9 ± 0.2	3.6 ± 1.0	90.6 ± 0.4	4.3 ± 0.7	100.8 ± 1.5	6.6 ± 0.9	106.6 ± 1.0
partially unfolded chromatin in dilute DM (10 mM Na^+)[b]	2.6	67.6	1.9	75.6	6.1	90.8	2.6	96.5	5.7	104.9
unfolded chromatin in dilute DM (10 mM Na^+)[c]	1.6 ± 0.4	63.4 ± 1.3	2.5 ± 0.2	74.5 ± 0.9	7.1 ± 0.6	90.5 ± 0.8	4.0 ± 0.5	97.6 ± 0.1	3.7 ± 0.2	103.5 ± 0.9
refolded chromatin in DM[c]	1.3 ± 0.4	63.9 ± 3.9	2.4 ± 0.5	74.0 ± 0.5	3.8 ± 1.0	90.0 ± 0.2	4.0 ± 0.5	98.6 ± 1.2	7.6 ± 1.1	107.0 ± 1.1

[a] The values are the mean of 10 determinations ± standard deviation. [b] The values are from the experiment shown in Figure 6B. [c] The values are the mean of five determinations ± standard deviation.

polyoma DNA occurs at 104 °C (Vinograd et al., 1968), these authors attributed the high-temperature transition of chromatin to supercoiled DNA and the passage of the transition enthalpy into the 90 °C endotherm to the relaxation of supercoiling as a consequence of strand cleavage. Obviously, the occurrence of a similar drift is foreseen whenever the DNA undergoes chain scission, but it must be stressed that what is detected by calorimetry is the higher order structure loss due to DNA damage rather than the loss of supercoiling. In fact, the altered thermal profile is observed at low ionic strength in the absence of breaks and reverts to the one of native chromatin by increasing the salt concentration.

That the net effect of variations in the ionic strength is an increase (or decrease) in the degree of condensation of chromatin cannot rule out a different explanation of the trends of the enthalpies of endotherms IV and V. It may be suggested that the ups and downs in the high-temperature region of the thermogram reflect a change in the denaturation mechanism which occurs when the ionic strength exceeds some critical value. However, the statement that the shape of the thermal profile is entirely determined by the conformation of chromatin implicates that the dominance of endotherm IV must be observed for unfolded chromatin at any ionic strength. The data reported in Figure 7, which are relative to calf thymus nuclei digested with trypsin, show that this is how matters stand. Under our digestion conditions (see Experimental Procedures), H1 is completely degraded, while core histones are cleaved to a set of limit peptides (Weintraub & van Lente, 1974; Allan et al., 1982). In the inset, these trypsin-resistant fragments are labeled according to the nomenclature of Weintraub and van Lente (1974). The removal of H1 and the cleavage of the basic tails of core histone permanently decondense chromatin, but the structural integrity of the nucleosome is maintained (Allan et al., 1982). The thermal profile of digested nuclei (scan a) compared with that of the control (scan b) shows a major endotherm at 90 °C and, as expected, only a residual thermal effect centered at 100 °C. However, it is apparent that this passage of transition enthalpy from V to IV is not the only consequence of the cleavage of the tails, because endotherm III broadens and ΔH^{III}_m increases with respect to native nuclei by 100%. In the concluding section, it will be shown that a comparable thermal behavior is observed in the case of intact nuclei at very low ionic strength (Figure 11) and this result provides evidence for the uncoiling of the core particle DNA, which increases the length of the linker. Ausio et al. (1989) recently established that the effect of trypsinization weakens the interaction of core DNA with the octamer. When detailed structural aspects are left out, this experiment conclusively shows that the denaturation of

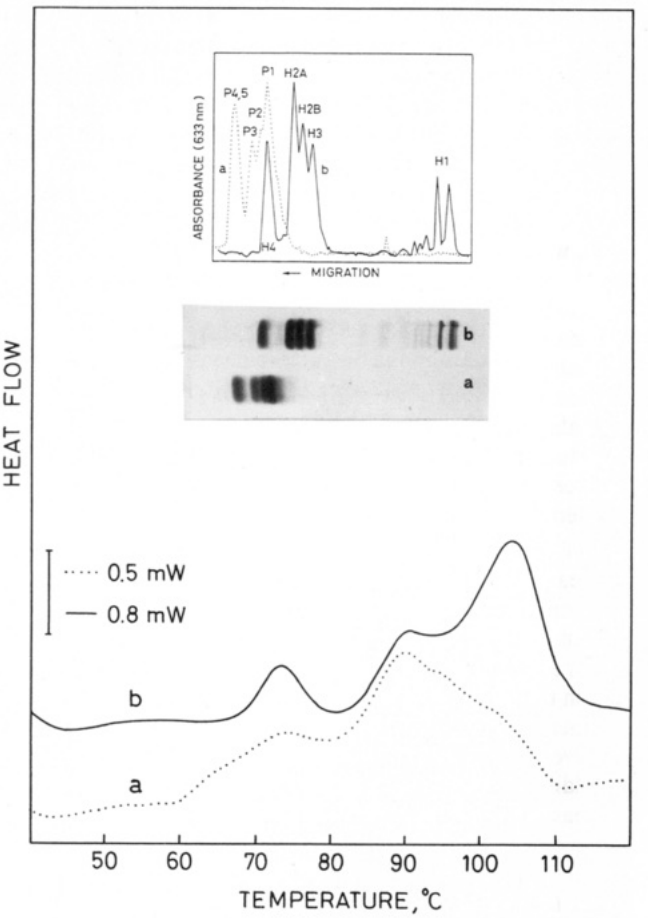

FIGURE 7: Effect of trypsin digestion on the DSC profile of calf thymus nuclei in DM. Nuclei were digested with 20 μg/mL trypsin at 4 °C for 1 h in DM and scanned at a rate of 10 °C/min (scan a). The thermal profile of control nuclei is shown for comparison (scan b). The inset shows 15% SDS–polyacrylamide gel analysis of the limit trypsin digest (a) and of the histone complement of control nuclei (b).

chromatin domains is determined by the strong interaction of DNA with histones over a wide range of ionic strength.

Stability of DNA in Chromatin. Separation of the Contributions of Assembly of the Polynucleosomal Chain and of Higher Order Folding. Starting from the data listed in Table I, we shall now address the problem of the forces responsible for the stability of the nucleosome and of the higher order structure. In fact, we measured the denaturation enthalpy of the polynucleosomal chain in both the extended and the condensed state (the 30-nm "solenoid" or "rope"), and from a comparison of the total transition enthalpy of chromatin with

the unstacking enthalpy of naked DNA, we can get an insight into the role of the interaction with histones. In the inset of Figure 10, we report the dependence of ΔH_m on T_m for hen erythrocytes and calf thymus DNA (Shiao & Sturtevant, 1973; Chipev & Angelova, 1983; this work). The slope of the plot is high, so that the transition enthalpy of the chromatin domains should be compared, as far as possible, with the value of ΔH_m of DNA determined at the same temperature. When transition 0, which arises from the unfolding of histones, as will be discussed in the following, is disregarded, for native calf thymus chromatin the denaturation of DNA occurs in endotherms III, IV, and V, with a total transition enthalpy equal to 16.3 ± 1.7 kcal·(mol bp)$^{-1}$, in agreement with the value previously determined for rat liver [15.4 ± 1.1 kcal·(mol bp)$^{-1}$]. In the case of fully unfolded chromatin in 10 mM Na^+, we obtain 17.2 ± 0.4 kcal·(mol bp)$^{-1}$. Thus, the denaturation enthalpy of DNA in chromatin does not change, within experimental error, as a consequence of unfolding. On the other hand, the correction which should be introduced on account of the increase (from 0.22 to 0.38) in the mole fraction of DNA melting in endotherm IV does not exceed 0.4 kcal·(mol bp)$^{-1}$, and can be neglected. The important consequence of this observation is that the conformational change of chromatin is an athermal process. Now, we can reasonably assume that all the DNA in unfolded chromatin melts at 90 °C (Figure 6C), with a transition enthalpy of the order of 17 kcal·(mol bp)$^{-1}$. At this temperature, the value of ΔH_m for naked DNA is equal to 9.1 kcal·(mol bp)$^{-1}$. Therefore, this approximate estimate yields a figure as high as 8 kcal·(mol bp)$^{-1}$ for the enthalpy of interaction between DNA and histones. In conclusion, the coiling of the DNA in the nucleosome is essentially enthalpy-driven, while its further folding in the higher order structure depends on entropy changes. This sharp demarcation between the roles of enthalpic and entropic forces can be related to structural features of the nucleosome.

In a previous work (Balbi et al., 1989), we observed a large decrease in the transition enthalpy when native nuclear chromatin from rat liver was unfolded by extensive digestion with micrococcal nuclease. This observation in itself can be taken as a strong indication in favor of an enthalpic contribution to the stability of the higher order structure arising from the interaction among nucleosomes. The results reported here, however, show definitely that, in the absence of DNA breaks, unfolding does not involve appreciable enthalpy changes. The decrease in the transition enthalpy as digestion progresses has, therefore, to be attributed to the increase in the enthalpy of the unordered polynucleosomal chain when it is fragmented down to the size of oligonucleosomes, and can reflect the relaxation of structural restraints in the nucleosome. Yau et al. (1982) have shown that the melting temperatures of the linker and core particle DNA increase by 3 and 2 °C, respectively, in going from dinucleosome to trinucleosome. The dependence of the stability of short chromatin fragments on the chain length can be very informative with respect to the energetics of the assembly of the 10-nm fiber and deserves further investigations.

The systematic investigation of the phase diagram in the Na^+/Ca^{2+} concentration plane (Widom, 1986) revealed striking competition effects between cations of different valence, in accordance with the theory of counterion condensation (Manning, 1969). We emphasize that, at least in the absence of divalent counterions, the equilibrium between the unfolded and folded states is entropy-driven, and therefore depends only on electrostatic forces. Within the frame of the molecular models for condensation, it is well established that the higher order structure is stabilized by both H1 and the binding of the highly charged N-terminal domains of core histones to DNA in adjacent nucleosomes (Allan et al., 1982). We have very recently found (Balbi et al., unpublished results) that when the tails are selectively removed with trypsin at physiological ionic strength, chromatin decondenses but the transition enthalpy is unaffected, the thermal profile being almost indistinguishable from the one of native chromatin unfolded at low ionic strength. This observation directly demonstrates that the salt linkages responsible for condensation are located within the hydrophilic domains.

The strong enthalpic stabilization of nucleosomal DNA cannot be reconciled with the hypothesis of a purely electrostatic interaction with the structural domains of core histones. The nature of the driving forces of the association process is at present unknown, although a dominance of hydrogen bonding represents a plausible interpretation. The same comment applies to a previous calorimetric investigation (Klump, 1976) on the stability of the complexes of DNA with poly(L-lysine). For the 1:1 complex, the transition enthalpy was found to be as high as 14.4 kcal·(mol bp)$^{-1}$. Bina et al. (1980) favored the opposing view that the stability of the nucleosome is primarily entropic in nature. These authors measured the denaturation enthalpy of the core particle in 0.25 mM EDTA. In this solvent medium, the main transition, involving 105 bp of DNA, occurs at 75.5 °C with ΔH_m equal to 13 kcal·(mol bp)$^{-1}$, which is higher than the unstacking enthalpy of the core particle DNA measured at the same temperature [9.2 kcal·(mol bp)$^{-1}$]. The difference was attributed to the denaturation heat of core histones, which was found to be equal to 4.83 cal·g^{-1} in 2 M NaCl. We believe that this value represents an overestimate; as will be discussed later on, the correct figure does not exceed 3 cal·g^{-1}. This discrepancy can be explained by considering the fact that in 2 M NaCl the histone octamer undergoes dissociation above 24 °C (Eickbush & Moudrianakis, 1978), a process which is strongly endothermic (Benedict et al., 1984). It is likely that extensive dissociation of the core has occurred in the calorimetric experiments of Bina et al. (1980), since the denaturation profile of the core particle in 2 M NaCl showed a complex series of endotherms over the temperature range 20–80 °C.

Application of IR Spectroscopy to Denaturation of the Nucleosome. Thermodynamic Analysis of the Melting of Structural Domains. The assessment of the general factors governing the stability of the polynucleosomal chain in the unfolded state can now be refined by evaluating the amounts of DNA which denature in each transition, and this information can be obtained by investigating the temperature dependence of the IR spectrum between 1400 and 1700 cm^{-1}. Since also the characteristic bands of the proteins occur within this region, the interrelation between the unfolding of histones and the unstacking of DNA can be directly established by this technique.

The temperature dependence of the IR spectrum of calf thymus nuclei in D_2O buffer (0.122 M NaCl, 0.5 mM Na_2-EDTA, and 10 mM Tris, pH meter reading 7) is shown in Figure 8. This solvent was used instead of DM in order to minimize the absorption of EDTA at 1620 cm^{-1}. The corresponding DSC profile is shown in Figure 9A. Only two endotherms, at 74.1 and 89.3 °C, are observed, the latter being slightly skewed to the right. Clearly, chromatin assumes an unfolded conformation in this medium. This somewhat unexpected result is due to a limited digestion process, since the DNA was found to be fragmented by agarose gel electrophoresis (lane b in the inset) while kept intact when nuclei

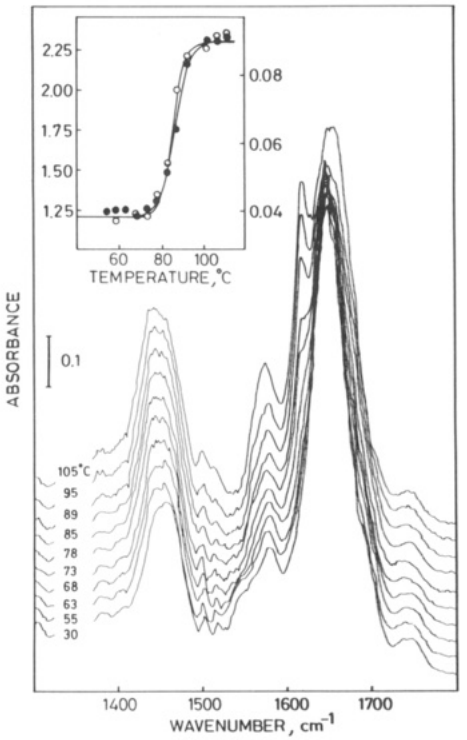

FIGURE 8: Temperature dependence of the IR spectrum of calf thymus nuclei in the 1300–1800 cm^{-1} region in D_2O buffer. The inset shows the thermal denaturation profile of calf thymus DNA in the same solvent, determined by measuring the ratio of the absorbances at 1665 and 1685 cm^{-1} (●, left ordinate) or the absorbance at 1625 cm^{-1} (○, right ordinate) as a function of temperature.

were stored in DM (lane a). Although we have found that the material isolated from calf thymus was less susceptible to DNA degradation than rat liver nuclei, nevertheless it is well-known that different Mg^{2+}/Ca^{2+}- or Mg^{2+}-dependent DNases are associated with calf thymus chromatin (Nakamura et al., 1981) and can therefore be activated whenever the concentration of EDTA drops below some critical value. Slightly digested chromatin is, of course, still the right material for the purpose of determining the amounts of DNA melting in transitions III and IV.

The IR spectrum of native chromatin shows the amide II′ band (largely ND bending) at 1450 cm^{-1} (Susi, 1969) and a complex absorption between 1600 and 1700 cm^{-1}, resulting from overlapping of the in-plane vibrations of the base residues (Tsuboi, 1964) and the amide I′ band (C=O stretching); Cotter and Lilley (1977) have shown that in this region the IR spectrum of the core particle is well approximated by the sum of the spectra of the DNA and of the octamer. The thermal denaturation of the DNA can be followed in two ways. One is based on the determination of the ratio of the absorbances at 1665 and 1685 cm^{-1}, which is directly correlated with the hyperchromicity at 260 nm (Kyogoku et al., 1961). Alternatively, the measurement of the increase in absorbance at 1625 cm^{-1} can be used (Fritzsche, 1971) since a band at this frequency has been assigned to the unpaired adenine residue (Tsuboi, 1964; Fritzsche, 1971). The inset in Figure 8 shows that the two methods yield the same denaturation curve for purified calf thymus DNA in D_2O buffer, with T_m equal to 87.5 °C. In the case of chromatin, the shift from 1685 to 1665 cm^{-1} is obscured by the strong amide I′ band at 1650 cm^{-1}, while the changes in the absorption which occur at 1625 cm^{-1} can be measured with high accuracy.

The percent hyperchromicity at 1625 cm^{-1} is plotted as a function of temperature in Figure 9B. The derivative melting

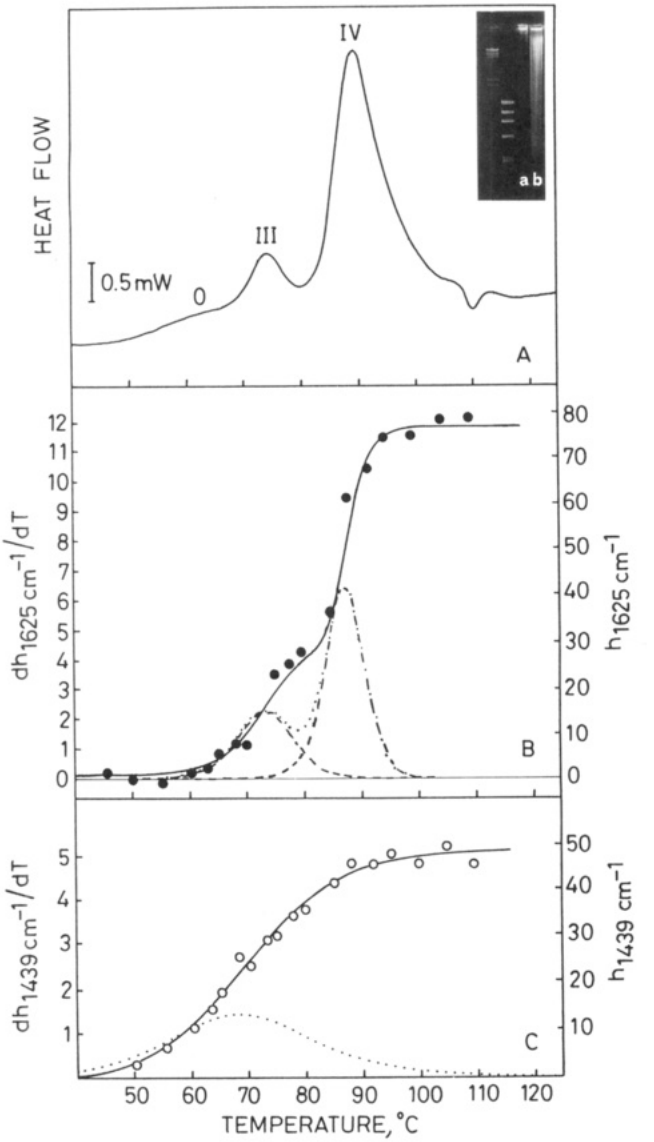

FIGURE 9: (A) DSC profile of calf thymus nuclei after a 6-h equilibration in D_2O buffer. The agarose gel electrophoretic pattern of DNA (lane b) shows the occurrence of a limited digestion process at variance with nuclei kept in DM (lane a). Size markers are as in Figure 4. (B and C) IR hyperchromicity of thermal denaturation at 1625 and 1439 cm^{-1} (solid line, right ordinate) and corresponding derivative curves (dotted line, left ordinate) of calf thymus nuclei in D_2O buffer.

profile is biphasic, with sharp maxima at 73.3 and 87 °C; comparison with the calorimetric scan shows that the DNA melts in endotherms III and IV, but not in 0. The areas under the component transitions are proportional to the amounts of denatured DNA, and we find that the contribution of transition III to the total hyperchromicity is equal to 33%. This estimate is in agreement with a previous value (30%) reported by Fulmer and Fasman (1979) for whole chicken erythrocyte chromatin but is somewhat higher than expected for the linker domain which correspond to 27% of the nucleosomal DNA. We note that the length of intercore DNA, as determined by the nuclease digestion probe, may not coincide with the length of the DNA segment involved in a single denaturation event; within the limits of resolution of the present method, the unstacking of the linker seems to propagate to 12 bp of core DNA. After deconvolution of the thermogram in Figure 9A (for the sake of clarity, the residual heat absorption between 90 and 110 °C has been attributed to endotherm IV) and normalization of ΔH_m^{III} and ΔH_m^{IV} [2.0 and 11.6 kcal·(mol

bp)$^{-1}$, respectively] for the fractions of DNA melting in each endotherm, we obtain 6.1 and 17.3 kcal·(mol bp)$^{-1}$. The latter value confirms our previous conclusions on the strong enthalpic stabilization of core particle DNA. The enthalpy of denaturation of the linker is, however, significantly lower than that of DNA at the same temperature [8 kcal·(mol bp)$^{-1}$].

The amide II′ band shifts to 1439 cm^{-1} with increasing temperature (Figure 8), a spectral change which is characteristic of the α-helix–random-coil transition (Miyazawa, 1962; Conio et al., 1971). By taking the derivative of the percent hyperchromicity at 1439 cm^{-1} as a function of temperature, we obtain a single broad transition at 67.7 °C (Figure 9C). Comparison with the low-temperature region of the DSC profile (Figure 9A) shows a close correspondence with transition 0, indicating that histones and the small amount of nuclear matrix proteins unfold in this endotherm. It must be pointed out that the determination of the values of the absorbance in this region of the IR spectrum is affected by the interference of trace amounts of HOD (Susi, 1969) and this circumstance has hampered the use of the amide II′ band in conformational investigations. In this work, however, we monitored the spectrum of the nuclear suspension as a function of temperature; the sample was heated in a tightly sealed cell, and as a consequence, contamination of the D_2O buffer did not appreciably occur during the experiments. Futhermore, the absorbance of the solvent is almost insensitive to changes in the temperature, so that our differential spectra must be considered highly reliable.

The low enthalpy of transition 0 [1.8 ± 0.5 kcal·(mol bp)$^{-1}$] can be explained by taking into account the structural features of the histone octamer and of H1. The DNA:total histones weight ratio is close to 1; hence, we obtain ΔH^0_m = 2.7 ± 0.8 cal·g^{-1}. This value is much less than that characteristic of compact globular proteins, at 65 °C, for which ΔH_m is between 6 and 8 cal·g^{-1} (Privalov, 1979). The variability of the specific enthalpy of proteins reflects differences in the proportion of folded regions. It is well-known that the histone molecules are only partially folded into compact domains. A recent reexamination of the secondary structure of core histone octamer by spectropolarimetry (Godfrey et al., 1990) showed that the α-helix and β-sheet contents are close to 53 and 5%, respectively. A more direct comparison can be made with the results of the calorimetric study of H1 by Tiktopulo et al. (1982). In 50 mM potassium phosphate containing 0.25 M K_2SO_4, this protein unfolds at 60 °C, with ΔH_m equal to 2.1 cal·g^{-1}. The compact domain of H1 was found to be 80 residues long. Although no precise estimate of the proportion of folded regions can be obtained by using a single determination of the transition enthalpy, the value of ΔH^0_m is compatible with the high content of unordered conformation of core histones.

In a recent paper, Almagor and Cole (1989c) have shown that the digestion with proteinase K of chromatin isolated from HeLa cells results in the disappearance of the transition at 73 °C, and consequently inferred that the core proteins denature at this temperature. It is, of course, equally legitimate to regard this result as a direct demonstration of the partition of the nucleosomal DNA between two structural domains, which vanish when the constraints imposed by histones are removed. Since the experiments were carried out in physiological salt conditions, no appreciable difference between the melting temperatures of core particle and naked DNA was observed, either transition occurring at 85 °C. Therefore, an effective answer could be obtained only by establishing whether or not the denaturation enthalpy at this temperature increases

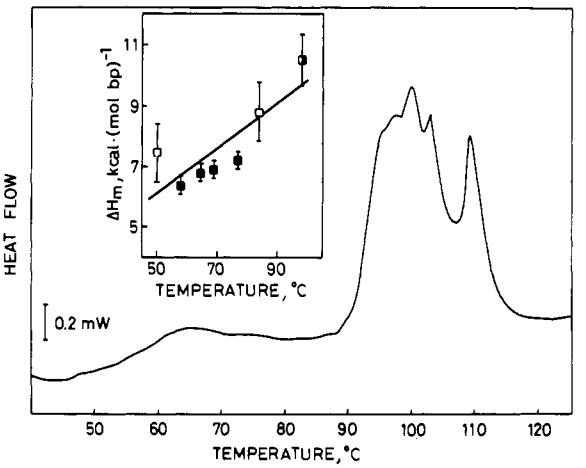

FIGURE 10: DSC profile of calf thymus nuclei in DM containing 2 M NaCl; scan rate, 10 °C/min. The inset shows the experimental dependence of the transition enthalpy of calf thymus and hen erythrocyte DNA on the transition temperature determined in the presence of different concentrations of Na^+ at neutral pH. Data from Shiao and Sturtevant (1973) (■) and Chipev and Angelova (1983) (□). The value in DM containing 2 M NaCl (◨) is from this work.

as a consequence of histone digestion. The data presented by these authors seem to rule out the occurrence of an enthalpy increase, but the specific transition enthalpy of chromatin after proteinase digestion was found to be equal to 6.76 cal·g^{-1} [4.37 kcal·(mol bp)$^{-1}$], which is just 50% lower than the best estimate of ΔH_m of DNA at 85 °C (inset in Figure 10). This discrepancy indicates that the determinations are affected by a quite large error, which prevents any quantitative conclusion to be drawn.

The assignment of endotherm 0 to the unfolding of histones can be verified in a remarkably simple way by determining the DSC profile of nuclei at an ionic strength high enough to dissociate the nucleohistone complex. The result is shown in Figure 10. When nuclei are equilibrated with DM containing 2 M NaCl, transitions III, IV, and V disappear and are replaced by the characteristic melting curve of calf thymus DNA centered around 99 °C. The sharp peaks superimposed on a broad main transition reflect the contributions of repetitive sequence (Blake & Lefoley, 1978; Lando et al., 1980). A broad endotherm having an enthalpy of 1.7 kcal·(mol bp)$^{-1}$ occurs at 65 °C. These values are well comparable with the thermodynamic parameters of transition 0 (Table I). As we have already noted, the dissociation of the histone core can introduce an additional enthalpic term. However, the major thermal effect is expected to arise from the unfolding of the isolated histone molecules, and the low value of the denaturation enthalpy supports in turn the view that the structure of the histone core is the same in the nucleosome and in high-salt solution.

Insight into the Thermodynamics of Wrapping of DNA around the Histone Core. From the above discussion, it is to be concluded that the conformational properties of DNA are strongly perturbed by the interaction with histones. The increase in the transition enthalpy of the core segment goes with the disappearance of the subtransitions characteristic of naked calf thymus DNA (Figure 10), and in the unfolded chromatin fiber, the unstacking of the duplex occurs in two widely separated, symmetrical endotherms. In this concluding section, we shall briefly consider the energetic aspects of the coiling of the DNA in the nucleosome by scrutinizing the dependence of the denaturation parameters of the structural domains on the ionic strength.

Calf thymus nuclei were equilibrated for 30 min at 25 °C

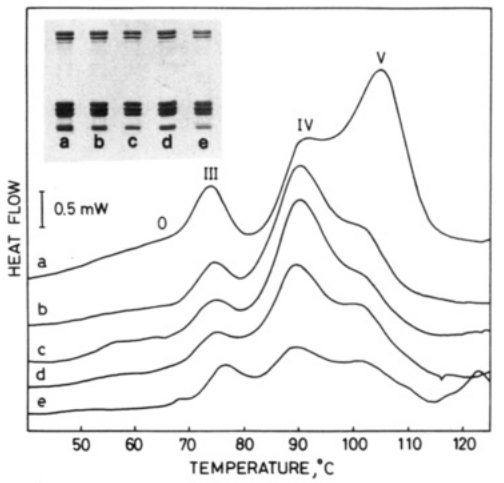

FIGURE 11: Effect of the counterion concentration on the DSC profile of unfolded nuclear chromatin. (a) Control calf thymus nuclei in DM (0.128 M Na^+); (b) 20 mM; (c) 10 mM; (d) 5 mM; (e) 1 mM. The corresponding electrophoretic patterns of the histone complement are marked by the same letter.

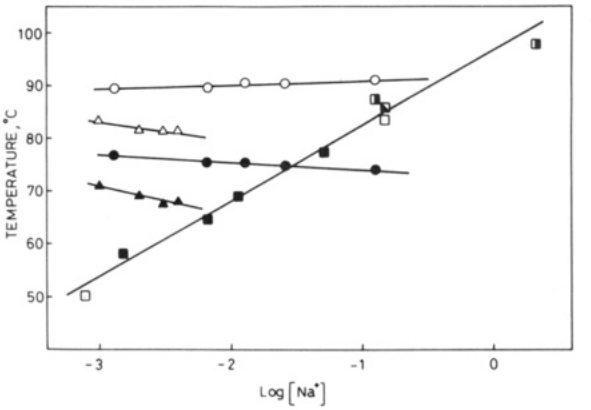

FIGURE 12: Dependence of the denaturation temperature of the structural domains of chromatin and of DNA on log [Na^+]. Transitions III and IV (●, ○) from this work. Linker and core particle DNA (▲, △) in chicken erythrocyte chromatin from Fulmer and Fasman (1979). Calf thymus DNA from Shiao and Sturtevant (1973) and Lando et al. (1980) (■, ◪). Calf thymus DNA from this work (◨). The value of T_m in the presence of 0.123 M Na^+ has been determined by IR spectroscopy. Hen erythrocyte DNA from Chipev and Angelova (1983) (□).

with dilute DM in the Na^+ concentration range 1–20 mM. The thermal profiles are shown in Figure 11. Under these experimental conditions, chromatin is expected to be in the unfolded state, and in fact, only a residual shoulder at 100 °C can be detected in all the scans. The characterization of the histone complement by 15% SDS–polyacrylamide gel electrophoresis is reported in the inset. It shows that neither appreciable degradation nor disproportionation has occurred as a consequence of the equilibration in dilute buffers. The isolated nuclear DNA did not enter 0.6% agarose gels, and had therefore a chain length higher than 48 kbp (data not shown). This result is not in contradiction with the occurrence of a digestion process in D_2O buffer (Na_2EDTA concentration 0.5 mM) since the complete exchange of protons requires several hours in order to be accomplished.

The major influence of the decrease in the counterion concentration is exerted on transition III. In going from 0.128 M to 1 mM Na^+, a continuous increase in T_m^{III} (from 73.9 to 76.5 °C) is observed (scans a–e). ΔH_m^{III} keeps a constant value down to 5 mM, but between 5 and 1 mM passes from 1.9 to 3.3 kcal·(mol bp)$^{-1}$. Thus, our calorimetric data agree well with the hyperchromicity study by Fulmer and Fasman (1978), which shows that the amount of DNA denaturing in the low-temperature transition increases sharply below 2 mM. The total transition enthalpy decreases in the limit of [Na^+] = 0, and in 1 mM, we obtain 13.3 kcal·(mol bp)$^{-1}$.

The diagram reported in Figure 12 shows the dependence of T_m on log [Na^+] (Balbi et al., 1989) of the linker and core particle DNA for both nuclear chromatin from calf thymus (endotherms III and IV) and whole chromatin isolated from chicken erythrocytes (Fulmer & Fasman, 1978). We note that T_m^{III} and T_m^{IV} are somewhat higher than the corresponding transition temperatures of chicken erythrocyte chromatin, since we are comparing the native nuclear material with fragments isolated by micrococcal nuclease digestion (Balbi et al., 1989). The denaturation temperatures of DNA from both calf thymus (Shiao & Sturtevant, 1979; Lando et al., 1980; this work) and hen erythrocytes (Chipev & Angelova, 1983) are plotted likewise. The (A+T):(G+C) ratios of these materials are very close (1.36 and 1.38, respectively; Malhes & Cordes, 1961) so that the dependence of T_m on the counterion concentration is the same within experimental error. The transition temperature of the different chromatin domains and of DNA plots varied linearly with log [Na^+]. However, it decreases slightly for the linker domain (closed circles) while in the case of DNA strongly increases (squares), according to the theoretical predictions. The fact that the slopes are of opposite sign has an important consequence. At low ionic strength, the linker melts at higher temperatures, as expected for a DNA segment with both ends clamped (Staynov, 1976). With increasing ionic strength, however, an intersection point occurs around 30 mM Na^+, and beyond this value, the linker will now be less stable than unprotected DNA. The puzzling decrease in the denaturation temperature of the linker in chicken erythrocyte chromatin (closed triangles) did not escape Fulmer and Fasman's notice, but no quantitative comparison with the melting of DNA is reported in their paper.

These data, taken together with the increase in ΔH_m^{III} below 5 mM Na^+, which has to be interpreted in terms of an increase of the length of the linker, indicate that the salt-dependent coiling of the DNA in the nucleosome induces a progressive destabilization of the segment which does not interact strongly with core histones. Very recently, Riehm and Harrington (1989), in order to monitor the thermal denaturation of chromatin at physiological ionic strength by UV hyperchromicity, developed a novel technique, based on the dispersion of the sample in polyacrylamide sols. At physiological ionic strength, the unstacking of the DNA occurred in two transitions at 83 and 63 °C. Since a decrease in T_m of 20 °C involves a free energy increase equal to 0.43 kcal·(mol bp)$^{-1}$, which is too high compared with an estimate of the free energy of bending of the DNA wrapped around the octamer, it was suggested that regions of the 30-nm fiber might be further destabilized by constraints imposed by the polyacrylamide matrix. Leaving out consideration of the adequacy of this circumstantial explanation, our results show that the premelt transition occurs independent of the formation of the 30-nm fiber and represents a general thermodynamic feature of the assembly of the nucleosome per se.

The evaluation of the bending free energy of nucleosomal DNA, taken to be a homogeneous chain characterized by the value of the persistence length (Riehm & Harrington, 1989), can be inadequate for the purpose of describing the real situation. Satchwell et al. (1986) have demonstrated that in chicken core particles long runs of homopolymer (dA)·(dT) are located near the ends of the DNA and suggested that the positioning of the octamer along the duplex can also be in-

fluenced by aversion of histones for sequences in the linker domain, for instance (dA)·(dT) and (dG)·(dC) blocks. A possible determinant of this aversion is the high flexural rigidity of these sequences, which opposes curvature (Drew & Travers, 1985). Following these authors, we interpret the anomalous dependence of T_m^{III} on counterion concentration as a manifestation of the resistance of the linker segment to bend in the direction dictated by the progressive coiling around the core. Although the path of the linker remains unknown, the best electron microscopic images of chromatin unfolded at low ionic strength (Thoma et al., 1979) show the presence of some helical (zigzag) structure, which can put additional constraints on the orientation of the duplex.

References

Allan, J., Harborne, N., Rau, D. C., & Gould, H. (1982) *J. Cell Biol. 93*, 285–297.

Almagor, M., & Cole, R. D. (1987) *J. Biol. Chem. 262*, 15071–15075.

Almagor, M., & Cole, R. D. (1989a) *Biochemistry 28*, 5688–5693.

Almagor, M., & Cole, R. D. (1989b) *Cancer Res. 49*, 5561–5566.

Almagor, M., & Cole, R. D. (1989c) *J. Biol. Chem. 264*, 6515–6519.

Ausio, J., Dong, F., & van Holde, K. E. (1989) *J. Mol. Biol. 206*, 451–463.

Balbi, C., Abelmoschi, M. L., Zunino, A., Cuniberti, C., Cavazza, B., Barboro, P., & Patrone, E. (1988) *Biochem. Pharmacol. 37*, 1815–1816.

Balbi, C., Abelmoschi, M. L., Gogioso, L., Parodi, S., Barboro, P., Cavazza, B., & Patrone, E. (1989) *Biochemistry 28*, 3220–3227.

Balbi, C., Barboro, P., Piccardo, M., Parodi, S., Cavazza, B., Brizzolara, G., & Patrone, E. (1990) in *Chemical Carcinogenesis 2: Modulating Factors* (Columbano, A., Feo, F., Pascale, R., & Pani, P., Eds.) Plenum Press, New York (in press).

Benedict, R. C., Moudrianakis, E. N., & Ackers, G. K. (1984) *Biochemistry 23*, 1214–1218.

Bina, M., Sturtevant, J. M., & Stein, A. (1980) *Proc. Natl. Acad. Sci. U.S.A. 77*, 4044–4047.

Blake, R. D., & Lefoley, S. G. (1978) *Biochim. Biophys. Acta 518*, 233–246.

Cavazza, B., Trefiletti, V., Pioli, F., Ricci, E., & Patrone, E. (1983) *J. Cell Sci. 62*, 81–102.

Chipev, C. C., & Angelova, M. I. (1983) *Int. J. Biol. Macromol. 5*, 252–253.

Conio, G., Patrone, E., & Salaris, F. (1971) *Macromolecules 4*, 283–288.

Cotter, R. I., & Lilley, D. M. J. (1977) *FEBS Lett. 82*, 63–68.

Dimitrov, S. I., Tsaneva, I. R., Pashev, I. G., & Markov, G. G. (1980) *Biochim. Biophys. Acta 610*, 392–399.

Drew, H. R., & Travers, A. A. (1985) *J. Mol. Biol. 186*, 773–790.

Eickbush, T. H., & Moudrianakis, E. N. (1978) *Biochemistry 17*, 4955–4964.

Fiers, W., & Sinsheimer, R. L. (1962) *J. Mol. Biol. 5*, 420–423.

Fritzsche, H. (1971) *Biochim. Biophys. Acta 228*, 344–349.

Fulmer, A. W., & Fasman, G. D. (1979) *Biopolymers 18*, 2875–2891.

Godfrey, J. E., Baxevanis, A. D., & Moudrianakis, E. N. (1990) *Biochemistry 29*, 965–972.

Johns, E. W., Goodwin, G. H. M., Hastings, J. R. B., & Walker, J. M. (1977) in *The Organization and Expression of the Eukaryotic Genome* (Bardbury, E. M., & Javaherian, K., Eds.) pp 3–19, Academic Press, New York and London.

Klump, H. (1976) *Biophys. Chem. 5*, 363–367.

Kyogoku, Y., Tsuboi, M., Shimanouchi, T., & Watanabe, I. (1961) *Nature 14*, 120–122.

Laemmli, U. K. (1970) *Nature 227*, 680–685.

Lando, D. Yu., Sinyakin, A. N., Fridman, A. S., Adrianov, V. T., & Akhrem, A. A. (1980) *Mol. Biol. (Engl. Transl.) 14*, 134–141.

Li, H. J. (1977) in *Chromatin and Chromosome Structure* (Li, H. J., & Eckhardt, R. A., Eds.) pp 37–69, Academic Press, New York and London.

Mahler, H. R., & Cordes, E. H. (1961) *Biological Chemistry*, Harper & Row Ltd., London.

Maniatis, T., Fritsch, E. F., & Sambrook, J. (1987) *Molecular Cloning. A Laboratory Manual*, 14th ed., Cold Spring Harbor Laboratory, Cold Spring Harbor, NY.

Manning, G. (1969) *J. Chem. Phys. 51*, 924–933.

Mirsky, A. E. (1971) *Proc. Natl. Acad. Sci. U.S.A. 68*, 2945–2948.

Miyazawa, T. (1962) in *Polyamino Acids, Polypeptides, and Proteins* (Stahmann, M. A., Ed.) pp 201–217, University of Wisconsin Press, Madison, WI.

Nakamura, M., Sakaki, Y., Watanabe, N., & Tagagi, Y. (1981) *J. Biochem. 89*, 143–152.

Nicolini, C., Trefiletti, V., Cavazza, B., Cuniberti, C., Patrone, E., Carlo, P., & Brambilla, G. (1983) *Science 219*, 176–178.

Panyim, S., Bilek, D., & Chalkey, R. (1971) *J. Biol. Chem. 246*, 4206–4215.

Privalov, P. L. (1979) *Adv. Protein Chem. 33*, 167–241.

Record, M. T., Jr., Lohman, T. M., & De Haseth, P. (1976) *J. Mol. Biol. 107*, 145–158.

Reuter, G., Giarre, M., Farah, J., Gausz, J., Spierer, A., & Spierer, P. (1990) *Nature 344*, 219–223.

Rice, S. A., & Doty, P. (1957) *J. Am. Chem. Soc. 79*, 3937–3947.

Riehm, M. R., & Harrington, R. E. (1989) *Biochemistry 28*, 5787–5793.

Satchwell, S. C., Drew, H. R., & Travers, A. A. (1986) *J. Mol. Biol. 191*, 659–675.

Seidl, A., & Hinz, H. J. (1984) *Proc. Natl. Acad. Sci. U.S.A. 81*, 1312–1316.

Seligy, V. L., & Poon, N. H. (1978) *Nucleic Acids Res. 5*, 2233–2252.

Shiao, D. D. F., & Sturtevant, J. M. (1973) *Biopolymers 12*, 1829–1836.

Staynov, D. Z. (1976) *Nature 264*, 522–525.

Susi, H. (1969) in *Structure and Stability of Biological Macromolecules* (Timasheff, S. N., & Fasman, G. D., Eds.) pp 575–663, Marcel Dekker, Inc., New York.

Thoma, F., Koeller, Th., & Klug, A. (1979) *J. Cell Biol. 83*, 403–427.

Tiktopulo, E. I., Privalov, P. L., Odintsova, T. I., Ermokhina, T. M., Krasheninnikov, I. A., Aviles, F. X., Cary, P. D., & Crane-Robinson, C. (1982) *Eur. J. Biochem. 122*, 327–331.

Touchette, N. A., & Cole, R. D. (1985) *Proc. Natl. Acad. Sci. U.S.A. 82*, 2642–2646.

Trefiletti, V., Balbi, C., Abelmoschi, M. L., Cavazza, B., Parodi, S., & Patrone, E. (1984) Abstracts of the 8th International Biophysics Congress, Bristol, U.K., Abstr. 22.

Tsaneva, I., Dimitrov, S., Pashev, I., & Tsanev, R. (1980) *FEBS Lett. 112*, 143–146.

Tsuboi, M. (1964) in *Conference on the Vibrational Spectra of High Polymers* (Natta, G., & Zerbi, G., Eds.) pp 125–137, Wiley, New York.
Vinograd, J., Lebowitz, J., & Watson, R. (1968) *J. Mol. Biol. 33*, 173–197.
Weintraub, H., & van Lente, F. (1974) *Proc. Natl. Acad. Sci. U.S.A. 71*, 4249–4253.
Weischet, W. O., Tatchell, K., van Holde, K. E., & Klump, H. (1978) *Nucleic Acids Res. 5*, 139–160.
Widom, J. (1986) *J. Mol. Biol. 190*, 411–424.
Yau, P., Thorne, A. W., Imai, B. S., Matthews, H. R., & Bradbury, E. M. (1982) *Eur. J. Biochem. 129*, 281–288.

Proton Homonuclear Correlated Spectroscopy as an Assignment Tool for Hyperfine-Shifted Resonances in Medium-Sized Paramagnetic Proteins: Cyanide-Ligated Yeast Cytochrome *c* Peroxidase as an Example†

James D. Satterlee,*,‡ David J. Russell,‡ and James E. Erman§
Department of Chemistry, Washington State University, Pullman, Washington 99164-4630, and Department of Chemistry, Northern Illinois University, DeKalb, Illinois 60115

Received April 25, 1991; Revised Manuscript Received July 3, 1991

ABSTRACT: Two types of homonuclear proton COSY experiments are shown to be useful in making resonance assignments in cyanide-ligated cytochrome *c* peroxidase, a 34 kDa paramagnetic heme protein. Both magnitude COSY and phase-sensitive COSY experiments provide spectra useful for making proton assignments to resonances of strongly relaxed hyperfine-shifted protons. This initial investigation demonstrates that COSY experiments combined with NOESY experiments are feasible for hyperfine-shifted protons of paramagnetic proteins larger than metmyoglobins and ferricytochromes *c*, for which the nuclear spin–lattice relaxation times are in the range 70–300 ms. Taken together, COSY and NOESY experiments, although not yet widely applied to paramagnetic metalloproteins, provide a reliable protocol for accurately assigning hyperfine-shifted resonances that are part of a metalloenzyme's active site. Specific examples of expected proton homonuclear COSY connectivities that were not observed in these experiments are presented, and utilization of COSY with respect to the proton resonance line widths and apparent nuclear relaxation times is discussed. The COSY experiments presented here provide valuable verification of previously proposed hyperfine resonance assignments for cyanide-ligated cytochrome *c* peroxidase, which were made by using NOESY experiments alone, and in several instances expand these assignments to additional protons in particular amino acid spin systems.

Application of two-dimensional NMR methods to paramagnetic metalloproteins has lagged behind its use in studies of diamagnetic molecules (Wuthrich, 1986). One reason for this may have been a perception that the comparatively short T_1's[1] and T_2's of nuclei demonstrating hyperfine-shifted resonances in paramagnetic molecules would severely compromise coherence transfer in COSY-type experiments and dipolar cross-relaxation in NOESY experiments. Recently, however, homonuclear bond-correlated spectroscopy and NOESY experiments have been explicitly demonstrated to be valuable for assigning rapidly relaxing hyperfine-shifted proton resonances in paramagnetic heme proteins (Yamamoto et al., 1989; Emerson et al., 1990; Busse et al., 1990; Yu et al., 1990; Gao et al., 1990; Satterlee & Erman, 1991).

The significance of these successes resides in the fact that for metalloproteins the active site frequently incorporates a paramagnetic metal ion. This results in strongly shifted, rapidly relaxed, broad resonances for protons in the active site, which are frequently the protons of primary interest in NMR studies. Despite the importance of those protons in biochemical studies, hyperfine resonance assignment methods have been slow to develop. This is possibly due to the observation that paramagnetism-induced effects on the NMR spectrum of active site protons compromise both direct elucidation of spin–spin coupling constants and commonly used chemical shift correlations, both of which are normally employed as starting bases for making assignments in diamagnetic molecules.

Literature reports show that whereas 2D bond-correlated spectroscopy has been utilized before in making assignments in small paramagnetic proteins, in most cases the assigned protons were typically main-chain and side-chain protons that were far removed from the paramagnetic center and therefore not extensively influenced by paramagnetic effects (Veitch et al., 1988; Feng et al., 1989; Feng & Englander, 1990; Gao et al., 1990; Veitch & Williams, 1990). In a few instances COSY experiments have been specifically used to assign hy-

† This work was supported by grants from the National Institutes of Health (DK30912, HL01758, and RR0631401, to J.D.S.), the National Science Foundation (DMB 8716459, to J.E.E.), and the Battelle Pacific Northwest Laboratories. We are grateful for this support.
‡ Washington State University.
§ Northern Illinois University.

[1] Abbreviations: CcPCN, cyanide-ligated cytochrome *c* peroxidase; CcP, native resting state cytochrome *c* peroxidase; HRP, native resting state horseradish peroxidase; HRPCN, cyanide-ligated horseradish peroxidase; 1D, one dimensional; 2D, two dimensional; T_1, nuclear spin–lattice relaxation time; T_1^{app}, apparent nuclear spin–lattice relaxation time; T_2, nuclear spin–spin relaxation time; NOE, nuclear Overhauser effect; NOESY, two-dimensional nuclear Overhauser effect spectroscopy; COSY, two-dimensional correlated spectroscopy; DQFCOSY, double-quantum filtered two-dimensional correlated spectroscopy; MCOSY, magnitude two-dimensional correlated spectroscopy; RCT, relayed coherence transfer.

0006-2960/91/0430-9072$02.50/0